

A REINTERPRETATION OF REGIONAL SEISMIC SURVEYS
IN NORTHERN ONTARIO AND EASTERN MANITOBA BETWEEN
DISTANCES OF 127 KILOMETERS AND 775 KILOMETERS
USING SEISMIC MODEL STUDIES OF THE CRUST AND UPPER MANTLE

A Thesis Presented to the
Faculty of Graduate Studies and Research
of
The University of Manitoba

In partial fulfillment
of the requirements for the degree
Master of Science

by
Ralph John Desmarais

May, 1976

**"A REINTERPRETATION OF REGIONAL SEISMIC SURVEYS
IN NORTHERN ONTARIO AND EASTERN MANITOBA BETWEEN
DISTANCES OF 127 KILOMETERS AND 775 KILOMETERS
USING SEISMIC MODEL STUDIES OF THE CRUST AND UPPER MANTLE"**

by

RALPH JOHN DESMARAIS

**A dissertation submitted to the Faculty of Graduate Studies of
the University of Manitoba in partial fulfillment of the requirements
of the degree of**

MASTER OF SCIENCE

© 1976

**Permission has been granted to the LIBRARY OF THE UNIVER-
SITY OF MANITOBA to lend or sell copies of this dissertation, to
the NATIONAL LIBRARY OF CANADA to microfilm this
dissertation and to lend or sell copies of the film, and UNIVERSITY
MICROFILMS to publish an abstract of this dissertation.**

**The author reserves other publication rights, and neither the
dissertation nor extensive extracts from it may be printed or other-
wise reproduced without the author's written permission.**

TABLE OF CONTENTS

	Page
LIST OF TABLES	ii
LIST OF FIGURES	vi
ABSTRACT	viii
ACKNOWLEDGEMENTS	x
INTRODUCTION	1
CHAPTER I. DESCRIPTION OF SEISMIC MODELS	4
Theoretical Time-Distance Curves	6
Theoretical Amplitude-Distance Curves	15
Discussion of Wave Types in Flat and Spherically Stratified Earth Models	21
Effect of Earth Curvature on Classical Velocity Determination Methods	27
CHAPTER II. APPLICATION OF MODEL RESULTS TO CRUSTAL DATA	36
Mid-range Survey of Hall-Hajnal	36
Long Range Survey of Gurbuz	38
Comparison of Data with Crustal Models	38
Reflection Multiples	48
Summary of Results	49
CHAPTER III. UPPER MANTLE MODELS	50
Existing Upper Mantle Research	50
Effect of Crustal Structure on Upper Mantle Events	52
Examination of Upper Mantle Models	54

CHAPTER IV.	INTERPRETATION OF UPPER MANTLE DATA	63
	Analysis of Velocities from Upper Mantle Data	
CONCLUSIONS		70
APPENDIX I.	DERIVATION OF DIX'S INTERVAL VELOCITY FORMULA	72
APPENDIX II.	DEVIATION OF $T^2 - X^2$ FROM STRAIGHT LINE FOR SPHERICAL EARTH - ONE LAYER CASE	77
APPENDIX III.	THEORETICAL VERTICAL AMPLITUDE DIS- PLACEMENTS FOR WAVES IN A PLANE LAYERED MEDIUM	79
APPENDIX IV.	PROGRAMS: HWAMP AND RDAMP	85
APPENDIX V.	PROGRAM: POLYFIT	94
APPENDIX VI.	PROGRAM: LSTSQR	102
APPENDIX VII.	PROGRAM: XTAMP	106
BIBLIOGRAPHY		137

LIST OF TABLES

		Page
Table Ia.	Crustal models A, B, C: Range of observation distances.	12
Table Ib.	Crustal models A, B, C: Arrival-time separation between reflections/refractions.	13
Table II.	Comparison of theoretical travel-times vs. distance between diffracted waves and body waves for crustal model A.	25
Table IIIa.	Polynomial fit to theoretical T^2-X^2 reflection curves: 120-360 km.	32
Table IIIb.	Polynomial fit to theoretical T^2-X^2 reflection curves: 420-780 km.	33
Table IIIc.	Polynomial fit to theoretical T^2-X^2 reflection curves: 0-800 km.	34
Table IV.	Distances and times for principal arrivals on records recorded in 1967, 1968 and 1969 (after Hall-Hajnal, 1973).	37
Table V.	Project Early Rise, July, 1966: University of Manitoba recording station data (after Gurbuz, 1970).	39
Table VIa.	Crustal refraction T-X data: Linear least squares fit.	44
Table VIb.	Crustal reflection T^2-X^2 data: Linear least squares fit.	47
Table VII.	Effect of crustal models A, B and C on upper mantle events.	53
Table VIII.	Upper mantle models: Comparison of travel-time curves of principal events.	57
Table IXa.	Upper mantle refraction T-X data: Linear least squares fit.	66

Table IXb. Upper mantle reflection T^2-X^2 data:
Linear least squares fit.

67

LIST OF FIGURES

		Page
Fig. 1.	Crustal models	5
Fig. 2a.	Crustal model A (reduced travel-times).	7
Fig. 2b.	Crustal model B (reduced travel-times).	8
Fig. 2c.	Crustal model C1 (reduced travel-times).	9
Fig. 2d.	Crustal model C2 (reduced travel-times).	10
Fig. 3a.	Amplitudes vs. distance of principal events: Crustal model A.	16
Fig. 3b.	Amplitudes vs. distance of principal events: Crustal model B.	17
Fig. 3c.	Amplitudes vs. distance of principal events: Crustal model C1.	18
Fig. 3d.	Amplitudes vs. distance of principal events: Crustal model C2.	19
Fig. 4.	Generation of interference head waves.	23
Fig. 5.	Amplitudes vs. distance for head waves and body waves: Crustal model A.	26
Fig. 6.	Average crustal and upper mantle model for Superior Province deduced from Project Early Rise records (after Gurbuz 1969, 1970).	40
Fig. 7a.	Upper mantle models containing first-order velocity discontinuities.	55
Fig. 7b.	Upper mantle models containing second-order velocity discontinuities.	56
Fig. 8a.	Amplitudes vs. distance of principal upper mantle events: Models 1.1 to 1.3.	60
Fig. 8b.	Amplitudes vs. distance of principal upper mantle events: Models 2.1 to 2.3.	61

Fig. A-1.	Ray-path geometry for two layer horizontally stratified media.	76
Fig. A-2.	Ray-path geometry for two layer horizontally stratified media.	76

ABSTRACT

Regional seismic refraction and wide-angle reflection surveys conducted in Manitoba and northern Ontario in recent years have resulted in similar but differing interpretations of structure in the Earth's crust and upper mantle. The present work was an attempt to determine, from a modelling study of the kinematic and amplitude characteristics of compressional reflected and refracted waves propagating in a spherically stratified earth, those events bottoming in the Earth's crust and upper mantle which would be most prominent on seismic records and the optimum range of observation distances at which the arrivals of these events could be observed.

It was found that the existence of positive vertical velocity gradients in a crustal layer would severely reduce the maximum observation distance of primary events bottoming in this layer. The loci of arrival-times versus distance of refracted and reflected waves bottoming in the same crustal layer were also found to converge with increasing distance thereby complicating resolution of the two events beyond certain distances. One class of reflection multiples was shown to produce events kinematically similar to primary reflections which could be misinterpreted for

the latter.

The model results were then used to re-interpret the seismic data derived from a short range (127-351 km.) survey by Hall and Hajnal in 1967-69 and a long range (427-775 km.) survey obtained by Gurbuz in 1966 which had resulted in conflicting interpretations.

The two data sets were found to conform to a single consistent crustal model, 34 km. in thickness, having an intermediate discontinuity at 18 km. with constant velocities of 6.05 km/sec. and 6.99 km/sec. respectively above and below the discontinuity. Both surveys led to the interpretation of a first-order discontinuity in the upper mantle at a depth of 50 km. with a compressional velocity of 8.17 km/sec. above the discontinuity. No unique compressional velocity was obtained for the layer below this interface. This may be attributable to lateral velocity variations over the survey area.

ACKNOWLEDGEMENTS

I wish to express my gratitude to Dr. D.H. Hall for his many helpful discussions. His guidance and direction were invaluable to the completion of this endeavour.

I am indebted to Dr. R.F. Mereu for allowing me the use of his computer program XTAMP written by him.

I would also like to thank Mr. M. Bonten for his assistance in drafting the diagrams.

Finally, I wish to thank Ms. K. Cohen for her long work in the preparation and typing of this manuscript and for her continuing support throughout this project.

INTRODUCTION

Since 1961, a number of seismic surveys have been conducted by the University of Manitoba Crustal Studies Group for the purpose of investigating crustal structure in the Churchill and Superior geologic provinces within Manitoba and Northern Ontario. A review of the published results from these surveys has been given by Hall and Hajnal (1973) together with the introduction and a preliminary interpretation of 24 new recordings made between 1967 and 1969.

The energy for these surveys was initiated by underwater explosions and recordings were made using a 12-detector one mile spread and analog tape recording. A complete description of the seismic instrumentation used by the group is given by Hajnal (1970).

With the exception of a long range refraction survey, which was part of Project Early Rise (Gurbuz, 1969, 1970), all of the work has led to an average crustal model containing two layers with bottom depths of 18.25 ± 4.8 km. and 34.28 ± 2.8 km. having constant compressional wave velocities of 6.05 ± 0.05 km./sec. and 6.85 ± 0.05 km./sec. respectively. This horizontally stratified model is based primarily on the travel times of identified primary wide-angle reflections and head waves with confirmation of depths obtained by the converted (head) wave method (Hall, 1966; Hall and Hajnal, 1969).

Gurbuz inferred a three layer, horizontally stratified

crustal model from the travel times of wide angle reflections and primary and converted head waves, whose identifications were supported by spectral amplitude ratios and phase angle spectra. The derived model has layer depths of 18 ± 3 km., 25.5 ± 3.5 km. and 34 ± 3 km. with P-wave velocities of 6.11 ± 0.01 km./sec., 6.81 ± 0.08 km./sec. and 7.10 ± 0.04 km./sec. Both Gurbuz and Hall and Hajnal report a velocity of 7.90 ± 0.05 km./sec. below the Mohorovicic discontinuity at the base of the crust.

A sub-Moho interface was also hypothesized by Gurbuz on the evidence of a primary reflection P_m and a head wave P_n , critically refracted at 46 km. and propagating below this discontinuity at an average velocity of 8.48 km./sec. As a result of this hypothesis, Hajnal's short range (110 km. - 156 km.) continuous refraction profile work was reexamined and events P_m and P_n were found on these records also, yielding a similar depth and velocity. These two events were also tentatively picked on recordings from the above mentioned 1967-69 mid-range regional survey.

The objective of the present thesis is threefold:

1. To investigate further the possibility of identifying events from an upper mantle discontinuity for distances comprising the range of existing deep crustal seismic records.
2. To determine, from a computer predictive modelling approach, those seismic events bottoming in the crust and upper mantle which would theoretically be most prominent on

a seismic trace and an optimum range of distances for which these events would be clearly distinguishable from one another. This knowledge of optimum shot point-receiver distances could be used when planning future refraction surveys to refine crustal and upper mantle structure.

3. Before the first problem can be approached, it is necessary to reconcile the apparently conflicting interpretations of two and three layer crustal models. The fact that Gurbuz does not report a reflection from the second layer at 25.5 km. has led to the suggestion (Hall and Hajnal, 1973) that a gradual increase in velocity with depth may take place between 18 km. and 34 km. and that this possibility may be consistent with both models. A two layer model containing a positive velocity gradient in the lower layer is therefore also considered in the following sections. In addition it has been found (Mereu, 1967; Mereu and Hunter 1969) that when the depth of a refractor exceeds 10 km., the effect of earth curvature becomes significant. Spherically stratified earth models have therefore been employed in the theoretical studies.

CHAPTER 1

DESCRIPTION OF CRUSTAL MODELS

It was recognized that an examination of the theoretical travel times and vertical amplitudes of seismic events associated with the two and three layer crustal models proposed in recent years is necessary. Figures 1a and b illustrate these two models and the ray paths of the compressional reflected and refracted waves produced in each. Model A contains a first order (Intermediate) discontinuity at 18 km. between the surface and the Mohorovicic discontinuity (34 km.) at the crustal base. Model B contains an additional first order discontinuity at 25.5 km. In an attempt to reconcile the conflicting interpretations, Model C (Figure 1), similar to Model A but containing a positive velocity gradient $b > 0$ in the lower layer, is also considered.

The following designation of compressional wave events will be used throughout this study:

For a two layer crust

- P1, P3, P5, etc. refer to refracted waves bottoming in the 1st, 2nd, and 3rd layer respectively.

- P2, P4, P6, etc. refer to reflected waves bottoming in the 1st, 2nd, and 3rd layer respectively.

-P2m, P4m, P6m, etc. are ray paths of waves which bottom and are multiply reflected once within the 1st, 2nd and 3rd layer, respectively.

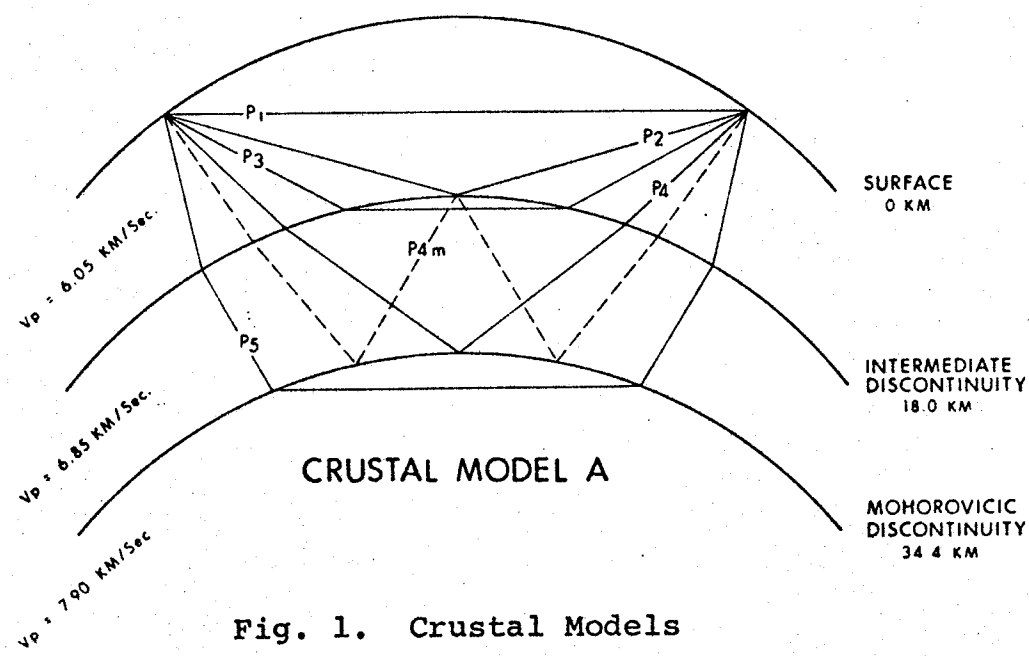
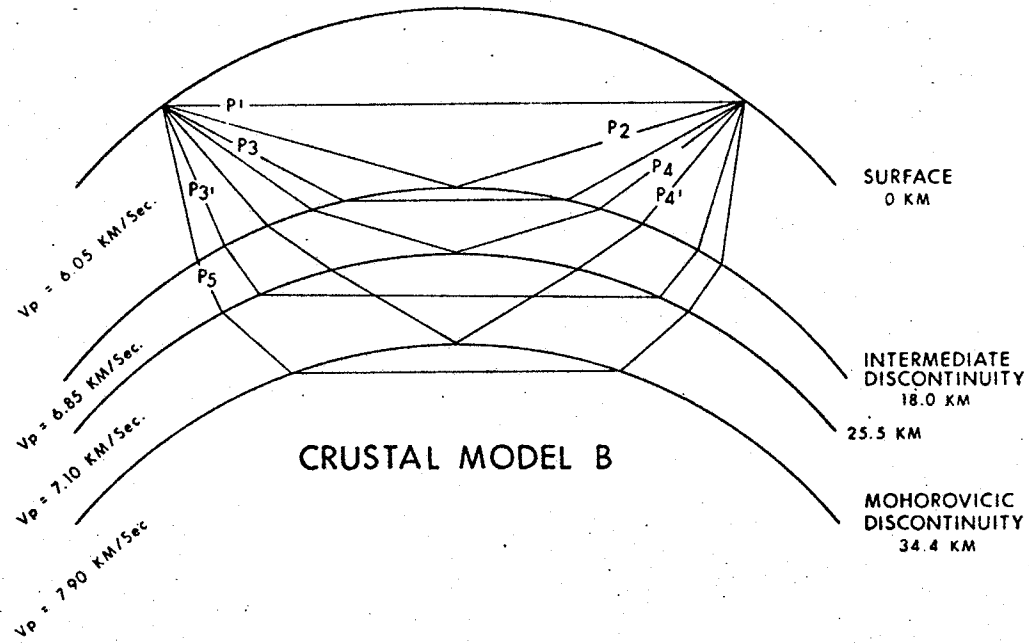
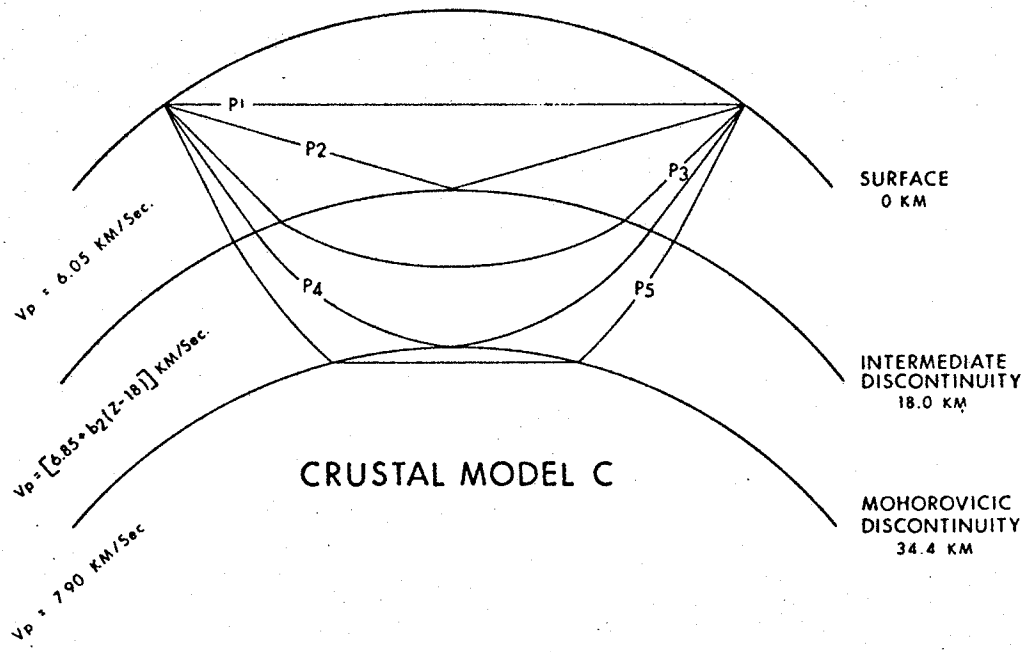


Fig. 1. Crustal Models

For a three layer crust

- the same notation as above will be used; events bottoming in the extra crustal layer, however, will be denoted by $P3'$, $P4'$, etc. (Figure 1 -Model C).

The refracted (body) waves existing in a spherical medium, unlike critically refracted (head) waves which propagate along the top of a constant-velocity layer, penetrate the bottoming layer to a depth dependent on the ray parameter p . As p decreases, the depth of bottoming Z_B and epicentral distance X increase for a refracted ray. The theory of head waves (Cf. Cerveny, 1967), based of the assumption of small distances over which earth curvature is negligible, has not been extended to account for interface curvature. A discussion on the amplitude and travel time characteristics of head waves versus those of body waves is given in Section 1.3.

1.1 Theoretical Time-Distance Curves

A computer program XTAMP (Appendix VII), written by R.F. Mereu, was used to calculate the theoretical travel times of primary events for a range of distances from 0-800 km. The program is based on a numerical solution by Stewart (1968) of the parametric integral equations given by Bullen (1963) for a ray travelling in a spherically stratified earth.

The following aspects of the travel time curves (Figures 2a-d) are common to all three crustal models:

- (a) Because of the curvature imposed on the layer

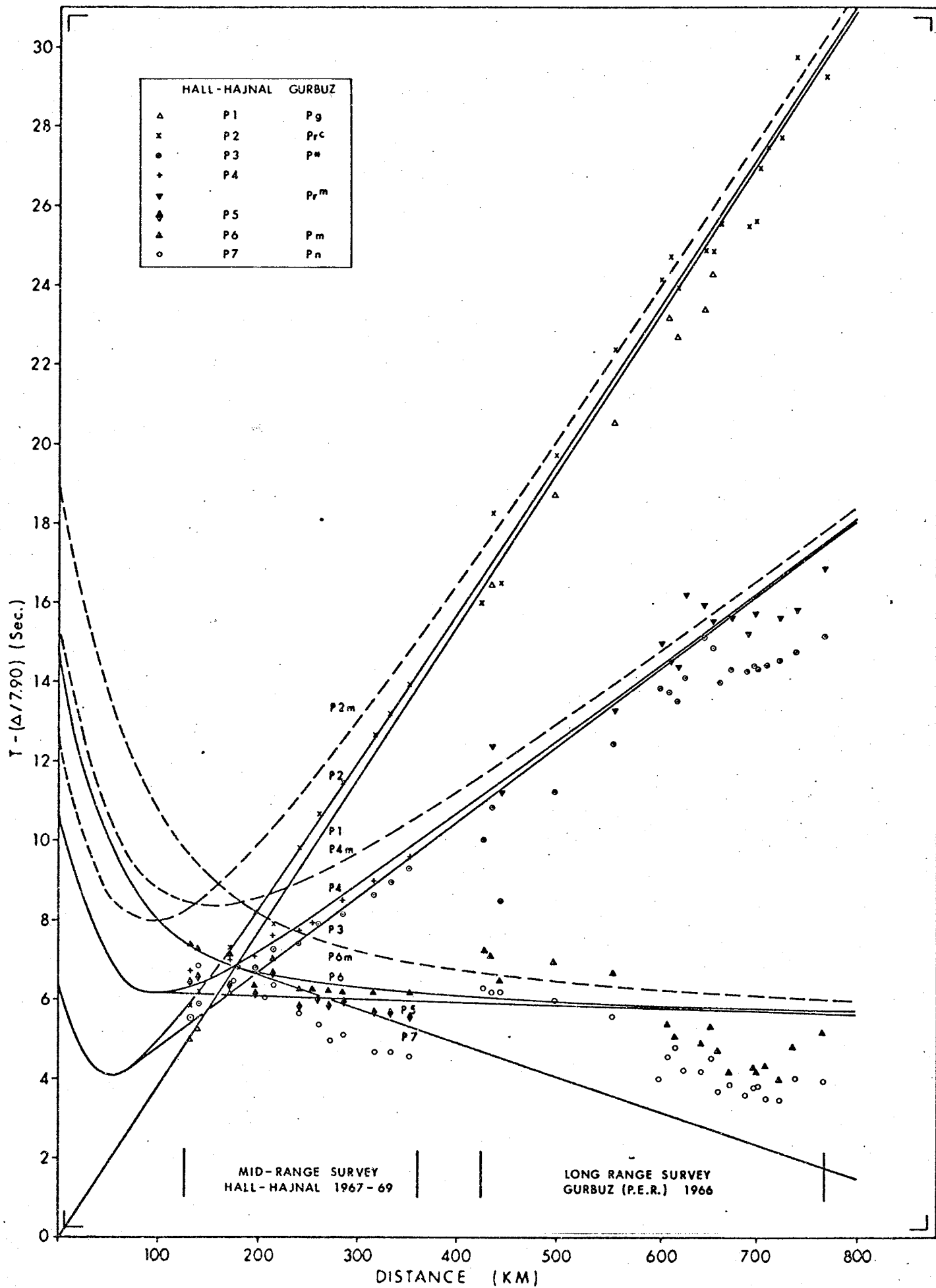


Fig. 2a. Crustal Model A (with upper mantle model 1.1)

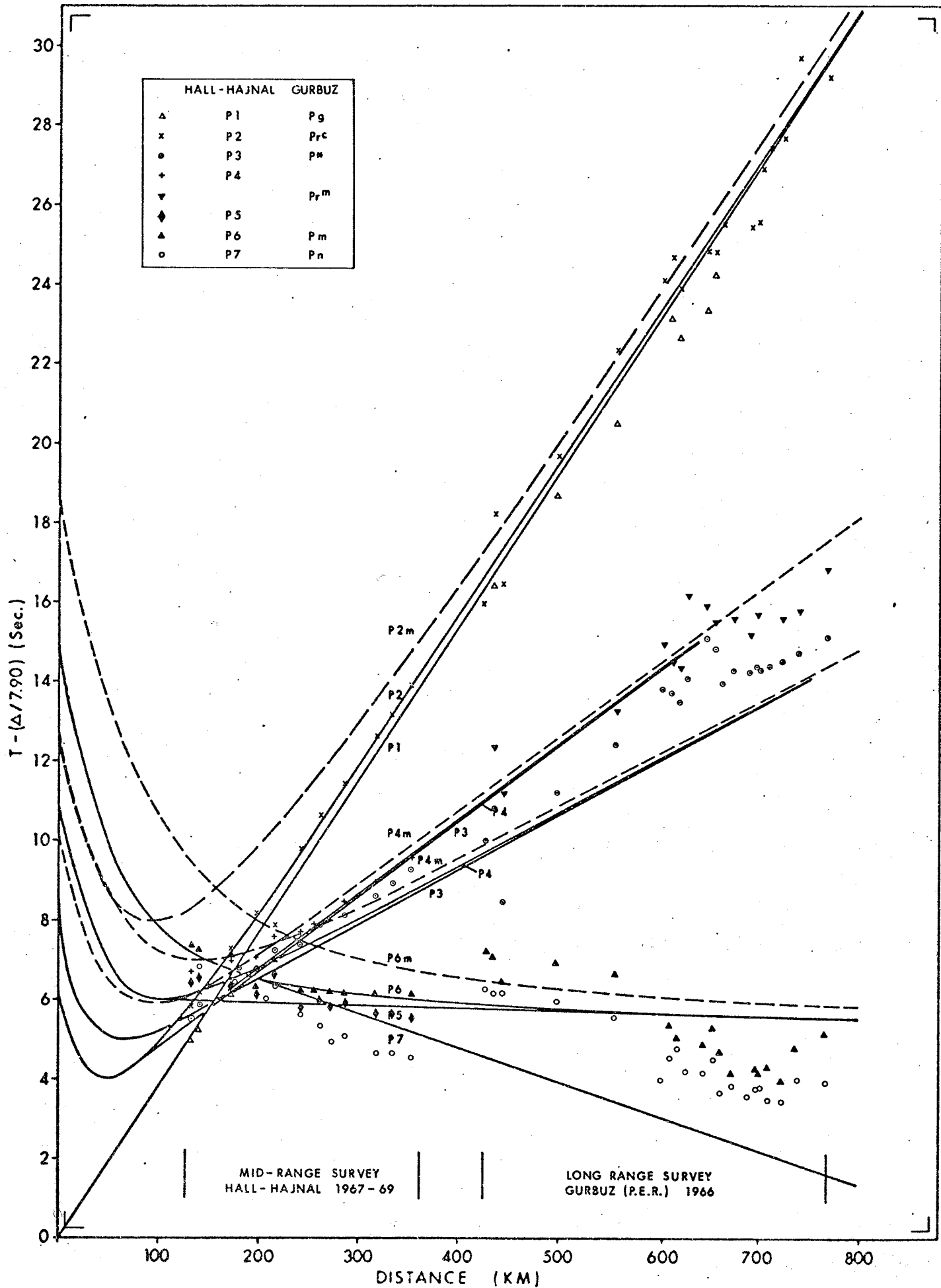


Fig. 2b. Crustal Model B (with upper mantle model 1.1)

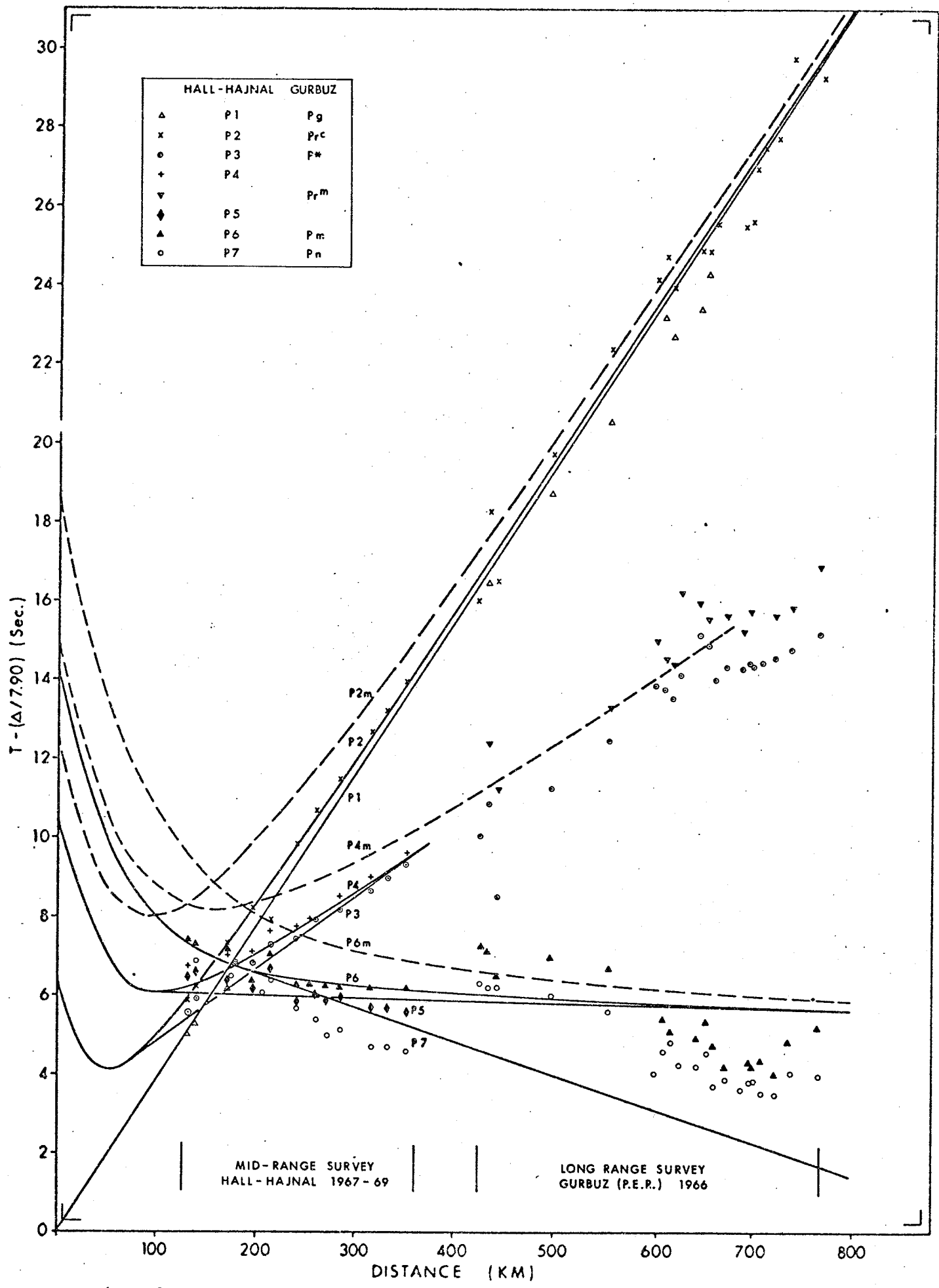


Fig. 2c. Crustal Model C1 (with upper mantle model 1.1)

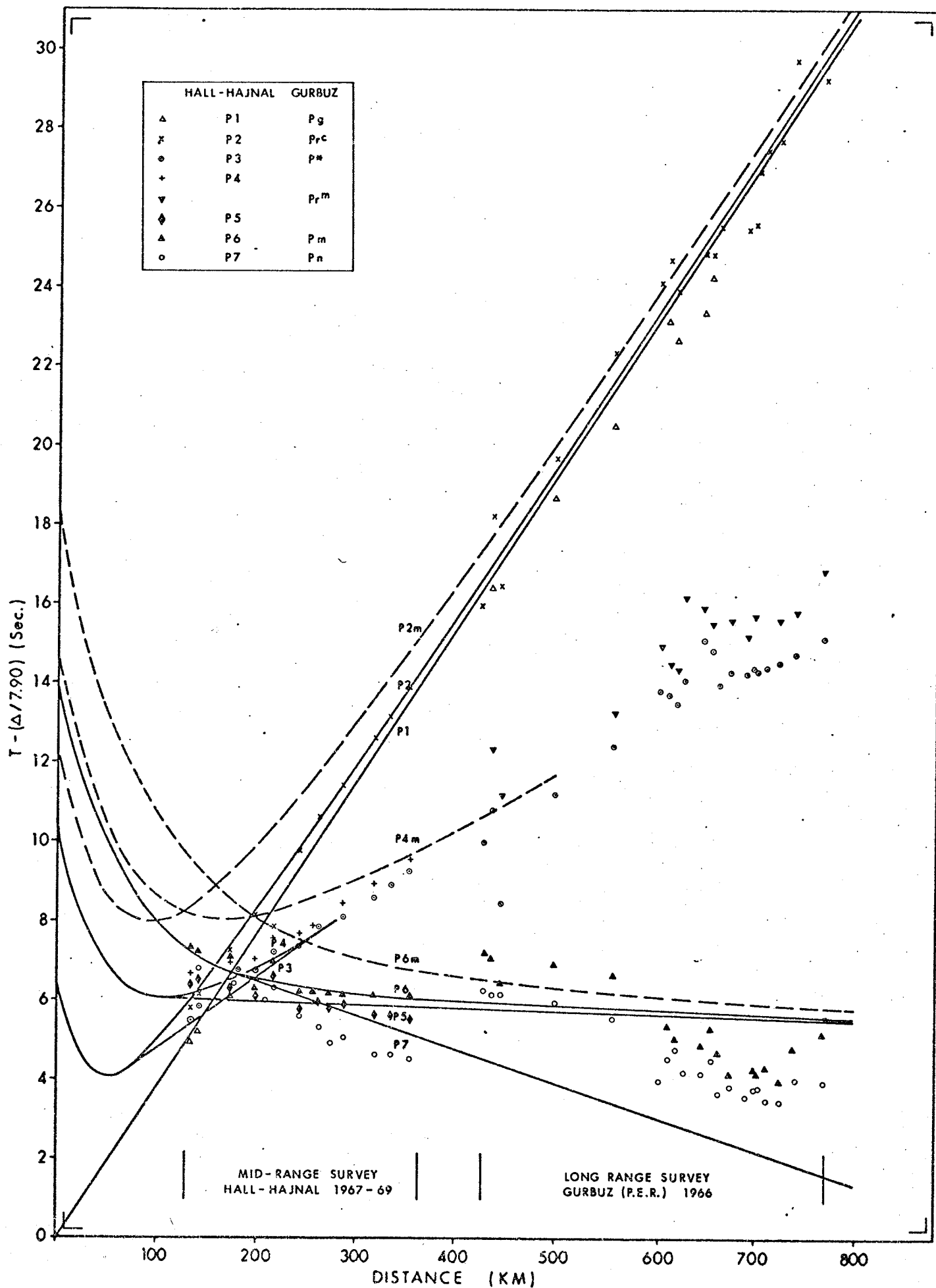


Fig. 2d. Crustal Model C2 (with upper mantle model 1.1)

interfaces, shadow zones are created at relatively short distances beyond which events no longer exist. The maximum distances of observation of all primary events are summarized in Table Ia. The thinning of a layer and/or the presence of a velocity gradient within a layer further reduce the maximum observation distance of events bottoming in it.

(b) For distances less than 60 km., only reflected events and the direct arrival exist. They are well separated in time and consequently their arrival times should be picked on records with relative ease. In the approximate range of 100-280 km. there is difficulty in distinguishing events from one another due to the onset of refracted waves and the convergence of all travel-time curves.

(c) Primary refracted and reflected events bottoming in the same layer (eg. P3 and P4) become asymptotic in time within the range of existing crustal survey distances. Table Ib shows the rate of convergence of these events for each model. This phenomenon has been cited (Lewis and Meyer, 1968) as a source of large error in first arrival measurements at large distances but its effect on later arrivals has largely been ignored. Pakiser and Steinhart (1964) using statistical information theory, conclude that for a S/N ratio of 2:1, first arrivals can be picked to

TABLE Ia
 CRUSTAL MODELS A, B, C
 RANGE OF OBSERVATION DISTANCES

CRUSTAL MODEL	CRUSTAL EVENTS			UPPER MANTLE EVENTS*		
	Event	Xmin (Km)	Xmax (Km)	Event	Xmin (Km)	Xmax (Km)
A	P1	0	958.2	P5	111.9	987.3
	P2	0	964.3	P6	0	987.3
	P3	85.0	936.6	P7	183.9	————†
	P4	0	936.6			
B	P3	85.0	640.9	P5	117.1	992.4
	P4	0	640.9	P6	0	992.4
	P3'	124.3	753.4	P7	186.8	————
	P4'	0	753.4			
C1 ($b_2 = 0.0072 \text{ sec}^{-1}$)	P3	72.28	374.9	P5	113.8	989.2
	P4	0	374.9	P6	0	989.2
				P7	185.0	————
C2 ($b_2 = 0.0156 \text{ sec}^{-1}$)	P3	70.05	274.7	P5	116.3	991.6
	P4	0	274.7	P6	0	991.6
				P7	186.4	————

* using average Upper Mantle model 1.1

† maximum distance dependent on possible existence of underlying refractor

TABLE I_b

CRUSTAL MODELS A, B, C*

ARRIVAL-TIME SEPARATION BETWEEN REFLECTIONS / REFRACTIONS

MODEL	EVENTS	MAXIMUM DISTANCE (Km) FOR T:		
		0.30 sec	0.20 sec	0.10 sec
A	P1:P2	286	354	522
	P3:P4	267	357	503
	P5:P6			
B	P3:P4	131	141	223
	P3':P4'	186	211	373
	P5:P6			
C1 ($b_2 = 0.0072 \text{ sec}^{-1}$)	P3:P4	208	240	265
	P5:P6			
C2 ($b_2 = 0.00156 \text{ sec}^{-1}$)	P3:P4	172	196	220
	P5:P6			

* using average Upper Mantle model 1.1

an accuracy of ± 0.03 sec.; for later arrivals they estimate a time uncertainty of ± 0.20 sec. or more. Resolving two events arriving this closely in time on a routinely processed record would therefore be virtually impossible.

Events P1 and P2, bottoming in the uppermost layer, whose properties are common to all crustal models investigated here, terminate at 964 km. The suite of time-distance curves of events bottoming below this layer, however, differs significantly for each model. The slopes of events P3 and P4 for Models A and B are the same since both have a bottoming-layer velocity of 6.85 km./sec.; the pair of events terminate at a much smaller distance (641 km.) in Model B, however, since its second layer is thinner than that of Model A. Furthermore, Model B produces an additional pair of primary events P3' and P4' (having an approximate inverse slope of 7.1 km./sec.), which bottom in the third crustal layer and also terminate at a relatively short distance of 753 km.

Model C, (having $b_2 > 0$) appears to fail as a compromise between the two- and three-layer constant velocity models. The imposition of a small gradient ($0 < b_2 < 0.001$ sec.⁻¹) shortens the termination distance of P3 and P4 but does not noticeably reduce the slope of their travel time curves from those of Model A. Larger gradients of 0.0072 sec.⁻¹ and 0.0156 sec.⁻¹ (Figures 2c and 2d) produce curves with smaller slopes (and correspondingly higher apparent velocities), but truncation at

very short distances of 375 km. and 275 km., respectively.

1.2 Theoretical Amplitude-Distance Curves

The theoretical vertical displacement amplitudes of compressional waves impinging on the free surface were calculated using programs XTAMP and HWAMP described in Appendices VII and IV. The former, written by R.F. Mereu, uses Guttenburg's (1944) method for the solution of the Zoepritz equations (Zoepritz, 1919) to calculate the transmission and reflection coefficients along a ray path in a spherical earth model; the latter program calculates the vertical amplitude of head waves as a function of distance for a plane layered medium based on a ray series solution developed by Cerveny (1971) according to the principles of geometrical optics.

The crustal amplitude curves (Figures 3a-d) were generated using an arbitrary source intensity equal to $10R_0^3$ where R_0 is the Earth's radius. In general, as expected, the largest amplitudes are exhibited by primary reflections which attain a maximum value at the critical distance X_c and decrease approximately as X^{-3} beyond X_c . Amplitudes of refracted body waves, bottoming in a constant velocity medium, however, increase with distance and, in the range of 700-800 km., exceed the amplitudes of reflected waves bottoming at underlying discontinuities.

This knowledge is crucial if amplitude ratios (between reflected and refracted waves) are used to support phase identifications based on arrival times since it was previously shown

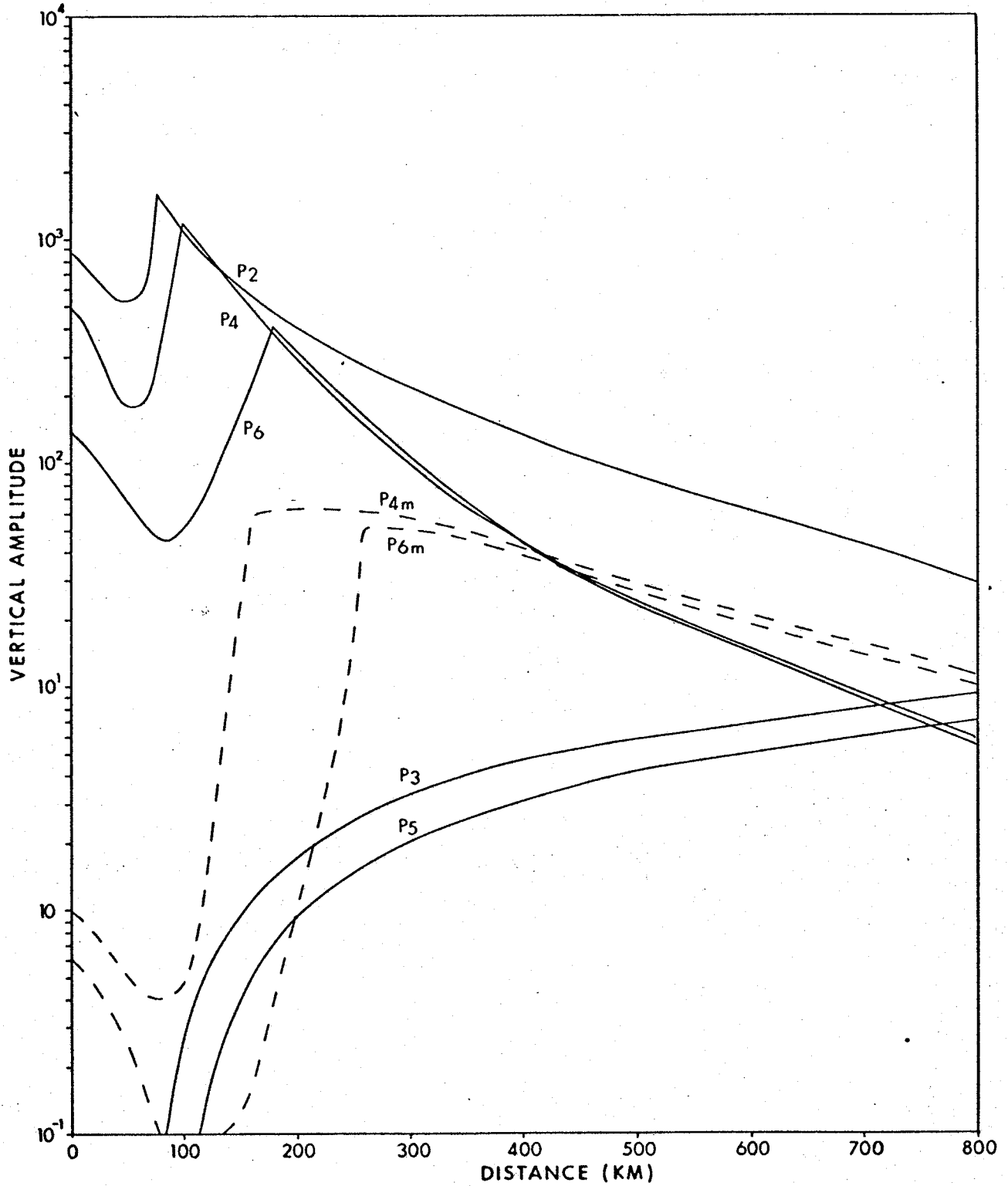


Fig. 3a. Amplitudes vs. distance of principal events:
Crustal Model A

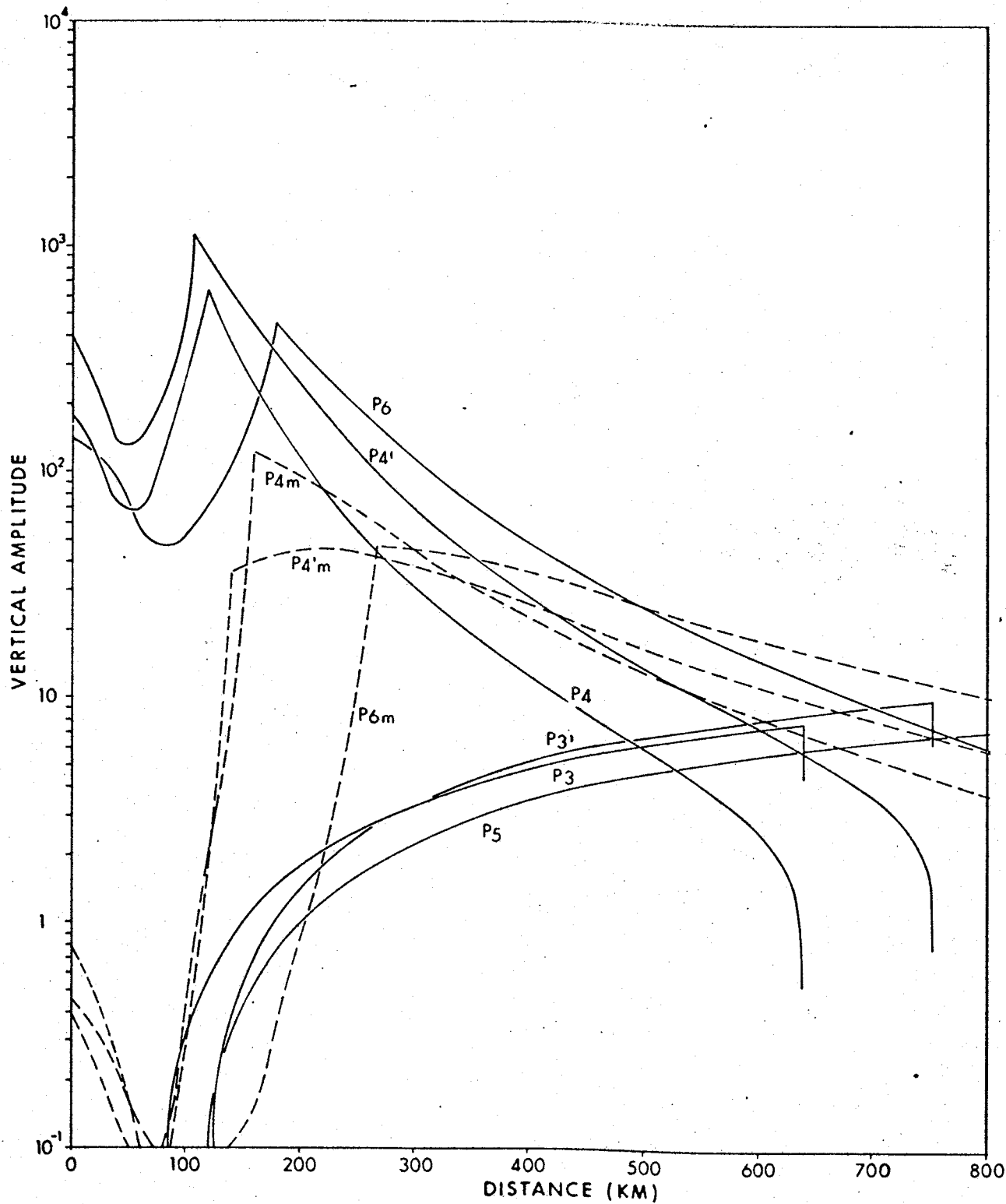


Fig. 3b. Amplitudes vs. distance of principal events:
Crustal Model B